Comparing finite volume and particle CFD simulation methods for understanding lubrication in automotive transmissions and axles

by Jin Xu[1,2], William W. Liou[1,2], and Yang Yang[3]

1. Department of Mechanical and Aerospace Engineering, Western Michigan University, USA
2. Computational Engineering Physics Lab, Western Michigan University, USA
3. Cook Research Incorporated, USA

Particleworks was 38.9 times faster than a finite volume approach. Particleworks ran on a quad-core PC with a GPU card and the finite-volume code ran on a 90-core CPU cluster.

Understanding the flow of oil lubrication in transmissions and axles is vital to improving their efficiency and reducing the wear of key components [1, 2]. Most geared transmissions and axles are splash lubricated, which means that lubrication of gears and bearings relies on complex flow patterns created by the gears churning the oil and the oil then deflecting off the walls of the gearbox housing. Appropriate levels of lubricant are required to keep all components lubricated [3, 4]. Lack of adequate lubrication where gears mesh and within the bearings will increase friction, leading to increased temperatures and premature failure of system components. Likewise, excessive lubrication can increase churning losses and reduce efficiency. Gearboxes generally operate conservatively with an excess supply of oil to improve operational reliability and gear life, but at the cost of operational efficiency. The choice, and volume of lubricant, and the shape of the gearbox housing can all be optimized for the expected gear speeds, loads, and temperatures. For example, lubricant viscosity varies with temperature. A low viscosity can cause excessive metal-to-metal friction between the gears during engagement, while high-viscosity lubricants can significantly increase the shear stress acting on the gear surfaces thus increasing the churning losses.

Computational fluid dynamics (CFD) simulations are widely accepted in the automotive industry as a method to understand lubricant flow progression within gearboxes and to optimize lubrication [5, 6]. CFD simulations represent a systematic and cost-effective method to study the performance of fluid-lubricated [7] or fluid-cooled devices under a wider range of operating conditions than could be tested using physical prototypes. CFD models based on finite volumes have been widely used to study gearbox lubrication and lubricant flow [8, 9]. Simulations focusing on lubricant flow give results that are in good agreement with experimental results [8, 10]. Currently, two main challenges limit the effectiveness of finite volume methods for simulating gearbox lubrication. First, the combination of the unsteady and turbulent nature of the flow and the need for some type of sliding or adaptive mesh to account for gear rotation can lead to computationally expensive simulations that may require prohibitively long simulation times on expensive hardware. Second, remeshing increases the technical skills a CFD engineer needs to achieve good results.

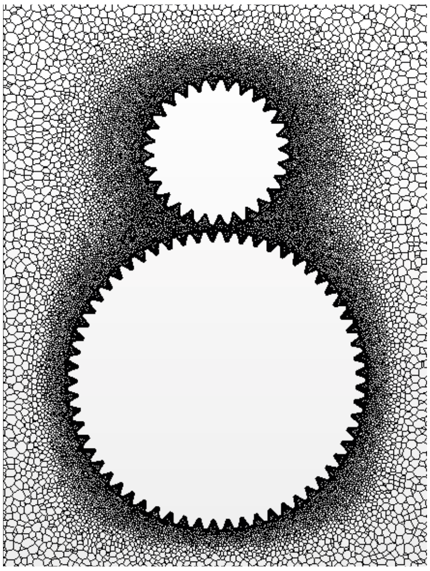

Fig. 1. Sliding mesh with 5.2M cells.

Particle-based CFD emerged in the 1970s in the form of smoothed-particle hydrodynamics [11] and later methods such as semi-implicit moving particle methods [12, 13]. The advantage of particle-based methods over finite-volume CFD methods [14, 15] is that remeshing is not required when free surfaces undergo drastic changes or when fluids coalesce or separate, which is commonly observed in lubrication flows.

The fluid mass represented by the particles can respond to moving boundaries as effectively as it does to stationary boundaries. Furthermore, CFD can be efficiently calculated on GPUs using meshfree particle methods. Modern advances in GPU technology allow CFD simulations with millions of particles to be calculated on a single GPU. This means that meshfree particle methods [16, 17] can handle complex gearbox geometries with the efficient use of computing resources. It has great potential for simulations involving free surfaces, such as lubricant oil flow simulations.

We compared CFD simulations using the finite volume (STAR-CCM+) and the meshfree particle (Particleworks) methods. The results show that both methods can be used to successfully understand lubrication and oil churning losses in the gearbox. However, in terms of calculation time, the Particleworks results are obtained much more efficiently.

Gearbox geometry and operating conditions

The internal dimensions of the example gearbox are 170mm (W) × 240mm (H) × 98mm (D). The larger of the two helical gears is the driving gear (or ring gear), which rotates clockwise (viewed from the front) at 3000rpm, as shown in Fig. 1. The driven gear (or pinion gear) has a corresponding rotational speed of 6535.7rpm. The top-land-to-top-land lengths for both gears are 118mm and 58mm, respectively. The lubricant level is 41.7mm from the lowest point of the ring gear, which is 22.21mm above the bottom of the gearbox interior. In other words, the lubricant filling depth is 63.91mm and the oil volume is 957cc. The effect of the friction between the lubricant and the gears on the oil temperature is not considered and it is assumed that the lubricant temperature is constant at 37.5°C. The corresponding lubricant density is 836.8kg/m^3 and the dynamic viscosity is 0.0281374Pa·s.

Simulation settings in STAR-CCM+

Finite volume-based simulations were performed using STAR-CCM+ [20] using the multiphase segregated flow solver and the realizable k-ε turbulence model [21], implemented with a constant time step of 2.5×10−5s. A sinusoidal ramp-up period of 0.01s was used to simulate the speed increase. A sliding mesh was used where a rotating sliding mesh shifts the mesh vertices of a region during the transient analysis of the rotating mesh. To apply the sliding mesh method, the upper gear (i.e. the pinion) was pulled upward by 4mm so that the closest (vertical) distance between the two gears was 2.25mm. Fig. 1 shows a two-dimensional (2D) representation of the mesh used in our simulation with 2.324 million (M), 0.504M and 2.343M cell elements for the ring gear refinement region, the pinion gear refinement region, and the remainder of the computational domain, respectively.

The total number of cells was 5.171M. Grid-independence studies were performed by varying the total number of cells from 1.7M to 5.2M and comparing the average churning loss. The largest difference in predicting the mean loss from two adjacent cell counts was less than 5%. The surface tension model was found to be negligible and was thus not included in the model. The simulations were performed with CPU-based cluster computing.

Simulation settings in Particleworks

Particle-based simulations were performed using Particleworks [22]. The large eddy simulation (LES) model was used for turbulence and the wall model was used to compensate for the lack of resolution near the wall in the LES model. The time interval (Δt) varies during the run and is defined as the minimum value of the initial time interval (set to 10−5s),

$$\frac{(\text{Courant }\#)\times(\text{Particle size})}{\text{Maximum velocity of particles}},\ \frac{(\text{Diffusion }\#)\cdot(\text{Particle size})^2}{\text{Maximum kinematic viscosity}}.$$

Smaller initial time intervals have been found to significantly increase the total number of time steps required for the simulation to reach a certain number of gear revolutions. The maximum peripheral speed of the gear was used to estimate the maximum particle velocity and was set to 30m/s. Particleworks simulations were performed using two particle counts: 0.95M with 1mm particles, and 1.87M with 0.8mm particles. To validate the computational speedup of the particle-based method running on a GPU, two computing platforms were compared: a multi-CPU workstation and a single GPU workstation.

STAR-CCM+ simulation results

The images in Fig. 2 demonstrate the temporospatial progression of the lubricant's volume fraction (VF) in the gearbox at four different instants of time, from 0.1s to approximately 0.7s (approximately 10.9–70.3 revolutions of the driven gear). While panel (a) is a 3D visualization of the flow behaviour in which the front wall is not visible, panel (b) provides a plan view of the axial median plane of the gear or the centre of the front and rear walls of the gearbox.

As the ring gear rotated clockwise, a significant amount of lubricant travelled along the port wall (seen from the front) with considerable accumulation in the corners adjoining the top wall, with occasional build-up on other walls. As the lubricant initially travelled along the port wall, it began to fall back down by about 0.16s (~17.4 revolutions of the driven gear). Also, at 0.15s (~16.3 revolutions of the pinion), the lubricant appeared to have passed over the top wall and started dripping along the starboard wall.

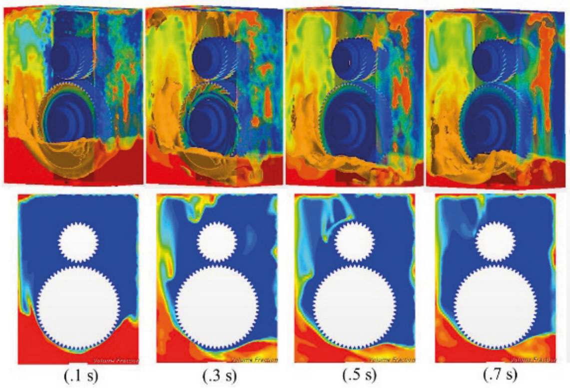

Fig. 2. Spatial progression of VF of lubricant predicted using STAR-CCM+.

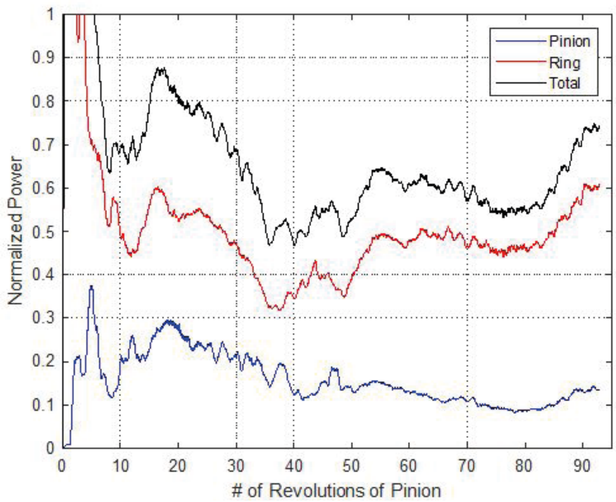

Fig. 3. Temporal history of churning losses for the two gears predicted using STAR-CCM+.

Fig. 3 shows the temporal history of normalized churning loss. Viscous force and pressure were considered in the calculation of churning losses. Since the gears were set to rotate at the target speeds at the beginning of the simulations, an initial transient occurred as the flow was responding to the sudden rotation of the gears.

The normalization parameter was chosen based on the value of the power loss after the initial transition of the simulated flow subsided. STAR-CCM+ predicted that the ring gear contributed about 80% of the total churning loss. Approximately 40% of the ring gear surface area was initially immersed in the lubricant pool.

The results show that the ring gear contributes significantly to the churning loss. The (normalized) average values of the pinion gear churning torque due to pressure and viscous forces were 4.79% and 6.84%, respectively. Furthermore, the counterparts of the ring gear were 19.63% and 28.12% due to pressure and viscous forces, respectively. It is worth noting that the viscosity mechanism played a more important role than pressure in terms of losses. The solution process was halted when the mass loss of the lubricant, common in similar simulations, exceeded 5% of the initial mass.

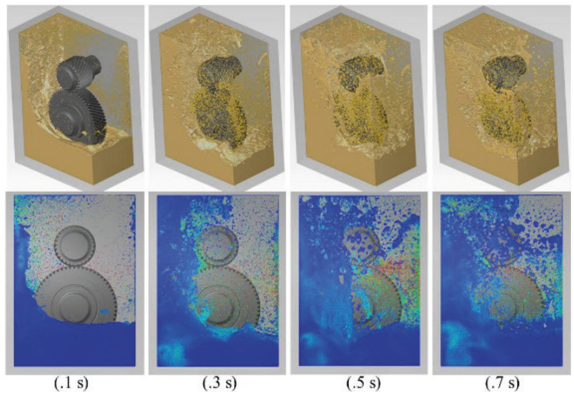

Fig. 4. Surface scene (top) and velocity scene (bottom) showing the lubricant progression predicted using Particleworks.

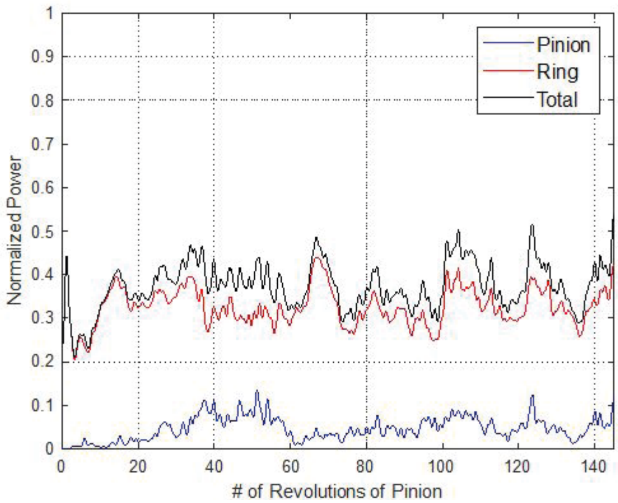

Fig. 5. Time history of predicted churning losses for the two gears using 1.87M particles.

Particleworks simulation results

Both a time-stepped velocity field and a surface formation were generated. Fig. 4 shows the simulation results for the same four moments as in Fig. 2 (0.1–0.7s and 10.9–70.3 pinion revolutions). While the maximum particle velocity may have exceeded the linear circumferential velocity (approximately 19m/s), the vast majority of particles moved far more slowly, justifying the use of an upper bound of 5m/s in the flow visualization. It would seem that the particle-based simulation was better able to capture cluster formation, fragmentation, and atomization.

Fig. 5 shows the time history of the churning losses calculated. Both viscous and pressure forces were taken into account. Similar to the STAR-CCM+ simulation results, the flow has an initial transient response to sudden gear rotation, and the contribution of the ring gear accounted for a considerable portion of the total churning loss.

Fig. 6 shows a breakdown of the contribution of pressure and viscous forces to the churning power loss on the ring gear and compares the results obtained using the two different particle counts (0.95M particles and 1.87M particles). The simulation ended at approximately 218 revolutions of the pinion gear i.e. 2s after the gears were moved. The trends in the evolution of power losses appear to be similar. The main contributor to the churning loss is the viscous force acting on the ring gear.

For the simulations of 0.95M and 1.87M particles, the values for the averaged total churning loss (sum of the viscous and pressure force contributions) are 0.353 and 0.341, respectively. Doubling the particle count resulted in a change of ~3.4% in the churning loss predicted, indicating that sufficient numerical accuracy was achieved with the use of 0.95M particles.

Calculation time result

It is interesting to evaluate the calculation time of the CFD simulations. While the simulations based on finite volumes were run

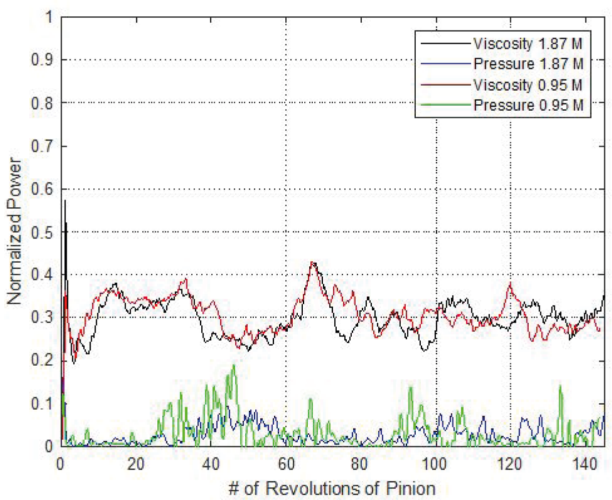

Fig. 6. Contribution to the ring gear power loss predicted using 0.95M and 1.87M particles.

Software	# of particles (million)	Particle size (mm)	Computing time/ Physical time (normalized to PW on GPU)	Average time (s) per step
PW on GPU	1.87	0.8	1	1.4
PW on CPU	0.95	1	10.6	16.0
PW on CPU	1.87	0.8	22.6	35.9
STAR-CCM+	N/A	N/A	38.9	N/A

Table 1. Comparison of computation times.

on a computer cluster with a 90-core CPU, the particle-based solver was run on two different computers: an 8-core CPU workstation and a GPU workstation. Only four cores were used for the CPU calculation.

Table 1 lists the computing performance in terms of computation time per unit of physical time. In physical time, the three particle-based CFD simulations required less solver time than their finite volume-based counterparts. The results also show that the computation time of the particle-based approach is proportional to the number of particles used in the simulation. For the same number of particles (1.87M), the simulation speed using the GPU workstation was 22.6 times faster than that using the quad-core CPU workstation, indicating that the particle-based approach is significantly faster for GPU computing.

Discussion and conclusion

Overall, the two simulation methods show good agreement. Both methods show flow patterns that are immediately recognizable visually in the other. Furthermore, the volume fraction measurements taken at different positions in the gearbox were in significant agreement, with two exceptions. Firstly, Particleworks seemed to be able to capture the lubricant build-up more easily, and dripping was observed from the middle of the top wall (see Fig. 7). Specifically, at 0.38s (corresponding to ~41.4 pinion revolutions), the dripping liquid counteracted the rotation of the pinion and increased the overall power loss. Secondly, the two simulations predicted different flow behaviours just outside the ring gear, with Particleworks predicting that a larger proportion of the oil would spread out from the ring gear to the wall.

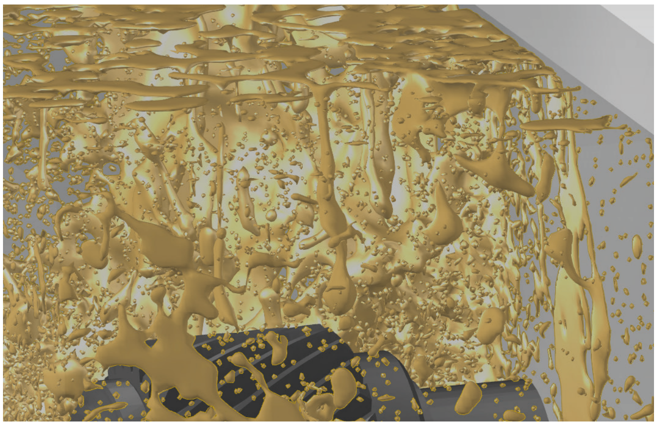

Fig. 7. Lubricant dripping from the middle of the top wall.

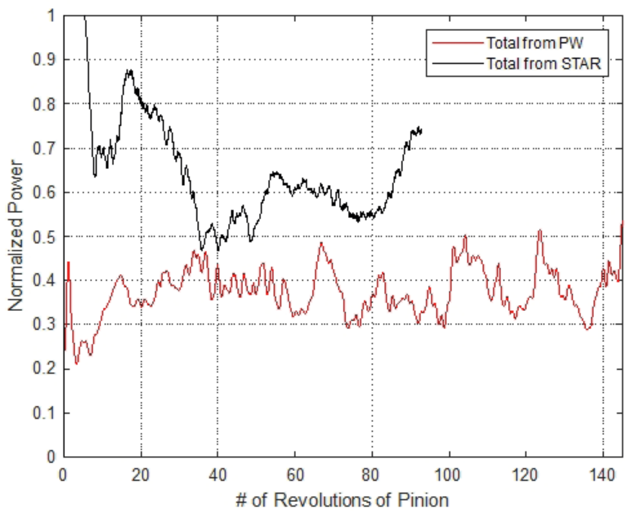

Fig. 8. Comparison of churning loss between Particleworks (PW) (1.87M particles) and STARCCM+ (STAR).

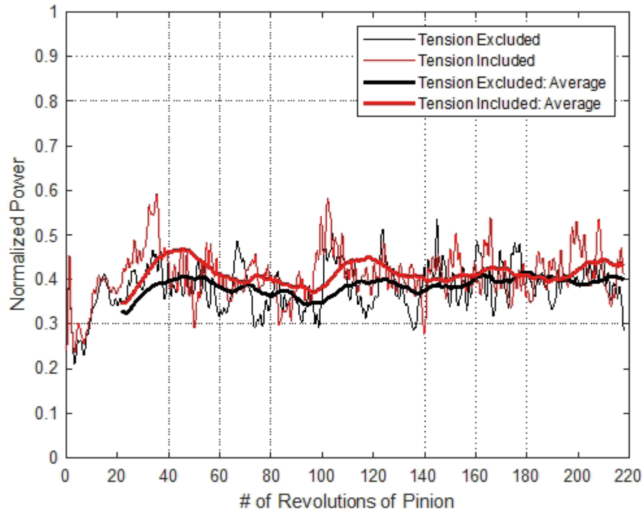

Fig. 9. Effect of surface tension on power loss per gear based on 1.87M-particle simulation results.

In Particleworks, the 0.95M- and 1.87M-particle simulations predicted globally similar flow behaviour in terms of churning power loss and local flow dynamics. The difference between the average values of total churning loss predicted by the two simulations was 3.4%. The lower particle-count simulation apparently provided the same level of resolution in terms of the averaged churning power loss.

Thus, the averaged churning loss is not sensitive to the two particle settings used in our simulations. It is also worth noting that while the power loss for both runs followed the same trend, the use of more particles seemed to suppress pressure-induced oscillations in the power-loss curve. The pressure-smoothing functionality is available but was not activated in the simulations.

The power loss due to gearbox oil churn obtained using both models is shown in Fig. 8. The churning loss calculated using the particle-based method fluctuates around the averaged value given above, indicating that the simulated flow could reach a state of statistical quiescence. Particleworks predicted that the ring gear churning contributes 86.2% of the total loss, compared to 79.1% in the STAR-CCM+ results. The simulation results of the two

CFD methods show that the ring gear contributes the most to the churning power loss.

For the particle-based method, the effect of surface tension modelling was further evaluated. The lubricating oil has a surface tension coefficient of 0.025N/m and a contact angle of 60°. The effect of surface tension on the churning power loss of the gears was examined separately and plotted in Fig. 9.

The loss pattern is similar with and without surface tension modelling. Oscillation characteristics are observed in the particle-based simulation results shown above, which seem to mask the general trend of transient changes in churning losses. A moving average with a time window of 0.2s was applied to the total churn loss to better observe the trends.

The results show that surface tension has no significant effect on the overall loss trend. Based on a window of 100 revolutions (from 120 to 220 revolutions, a smooth statistical flow was obtained), the average value excluding surface tension was 0.395, which is 4.88% lower than when surface tension was included. The Particleworks results without surface tension modelling were used for the comparison with the STAR-CCM+ simulation results in the Results section.

CFD is widely used in the automotive industry, and simulation time and optimization of CFD modelling remain a significant challenge. The results presented illustrate the difference in computational efficiency between two CFD software programs that are used to simulate gearbox lubrication.
While finite-volume methods have a longer history, particle-based methods have proven their value in capturing flow behaviour, enabling faster simulation of transient free-surface flows such as those in oil lubrication.

Acknowledgments

This work was supported in part by the CAViDS Consortium at Western Michigan University. Thanks to Carlos Wink of Eaton Corp., and Andrea Lucci, Mark Williams, and Dakota Dawson of Dana Inc. for hardware and application software support. Technical assistance was provided by Zach Smith and Dr. Brant Ross of EnginSoft USA.

For more information:
James Crist - EnginSoft USA
j.crist@enginsoft.com

References

[1] A.S. Kolekar, A.V. Olver, A.E. Sworski, and F.E. Lockwood, "Windage and Churning Effects in Dipped Lubrication", *Journal of Tribology*, 136, no. 2, 2014: 021801.

[2] P.M.T. Marques, C.M.C.G. Fernandes, R. Martins, and J.H.O. Seabra, "Power Losses at Low Speed in a Gearbox Lubricated with Wind Turbine Gear Oils with Special Focus on Churning Losses", *Tribology International*, 62, 2013, pp. 186–197.

[3] S. Seetharaman and A. Kahraman, "Load-independent Spin Power Losses of a Spur Gear Pair: Model Formulation", *Journal of Tribology*, 131, no. 2, 2009: 022201.

[4] S. Seetharaman, A. Kahraman, M.D. Moorhead, and T.T. Petry-Johnson, "Oil Churning Power Losses of a Gear Pair: Experiments and Model Validation", *Journal of Tribology*, 131, no. 2, 2009: 022202.

[5] C. Gorla, F. Concli, K. Stahl, B.R Höhn et al, "CFD Simulations of Splash Losses of a Gearbox", *Advances in Tribology* 2012, 2012, pp. 1–10.

[6] C. Changenet and P. Velex, "A Model for the Prediction of Churning Losses in Geared Transmissions — Preliminary Results", *Journal of Mechanical Design*, 129, no. 1, 2007, pp. 128–133.

[7] F. Concli, C.T. Schaefer, and C. Bohnert, "Innovative Meshing Strategies for Bearing Lubrication Simulations", *Lubricants*, 8, no. 46, 2020, pp. 1–14.

[8] H. Liu, T. Jurkschat, T. Lohner, and K. Stahl, "Determination of Oil Distribution and Churning Power Loss of Gearboxes by Finite Volume CFD Method", *Tribology International*, 109, 2017, pp. 346–354.

[9] H. Liu, T. Jurkschat, T. Lohner, and K. Stahl, "Detailed Investigations on the Oil Flow in Dip-Lubricated Gearboxes by the Finite Volume CFD Method", *Lubricants*, 6, no. 2, 2018, pp. 47.

[10] T. Noda, K. Shibasaki, S. Miyata, and M. Taniguchi, "X-Ray CT Imaging of Grease Behavior in Ball Bearing and Numerical Validation of Multi-Phase Flows Simulation", Japanese Society of Tribologists, 15, no. 1, 2020, pp. 36–44.

[11] M. Sasson, S. Chai, G. Beck, Y. Jin et al, "A Comparison between Smoothed-Particle Hydrodynamics and RANS Volume of Fluid Method in Modelling Slamming", *Journal of Ocean Engineering and Science*, 1, 2016, pp. 119–128.

[12] S. Koshizuka and Y. Oka, "Moving-Particle Semi-Implicit Method for Fragmentation of Incompressible Fluid", Nuclear Science and Engineering, 123, no. 3, 1996: 282420.

[13] M. Galbiati, "Oil Splashing, Lubrication and Churning Losses Prediction by Moving Particle Simulation", presented at the NAFEMS World Conference 2017, June 2017.

[14] F. Concli, "Numerical Modelling of the Churning Power Losses of Gears: An Innovative 3D Computational Tool Suitable for Planetary Gearbox Simulation", *Tribology International*, 103, 2013, pp. 58–68.

[15] L. Martinelli, M. Hole, D. Pesenti, and M. Galbiati, "Thermal Optimisation of e-Drives Using Moving Particle Semi-Implicit (MPS) Method", EnginSoft *Newsletter*, Year 15, no. 3, pp. 27–33.

[16] T. Iino, S. Matsumura, H. Houjoh, and T. Haciya, "Calculation of the Behavior of Oil Churning and its Loss in a Gear Box by a Moving Particle Method: The First Result of Both Calculation and Experiment", *Power Transmissions*, D. Qin and Y. Shao (Eds) (London: Taylor & Francis Group, 2017), ISBN:978-1-138-03267-5.

[17] M. Haga and T. Kasahara, "Simulation of Oil Separating Behavior for Engine Breather System", Honda R&D Technical Review, 26, no. 2, 2014, pp. 98–106.

[18] P. Norman and K. Howard, "Evaluating Statistical Error in Unsteady Automotive Computational Fluid Dynamics Simulations", SAE Technical Paper, 2020-01-0692, 2020, <doi.org/10.4271/2020-01-0692>.

[19] H. Tennekes and J.L. Lumley, *A First Course in Turbulence* (Cambridge, MA: MIT Press, 1972), pp. 197–221, ISBN:978-0- 262-20019-6.

[20] <www.plm.automation.siemens.com/global/en/products/simcenter/STARCCM.html>, accessed.

[21] T.H. Shih, W.W. Liou, A. Shabbir, Z. Yang et al, "A New k-e Eddy Viscosity Model for High Reynolds Number Turbulent Flows", *Computers & Fluids*, 24, 1995, pp. 227–238.

[22] Y. Chikazawa, S. Koshizuka, and Y. Oka, "A Particle Method for Elastic and Visco-Plastic Structures and Fluid- Structure Interactions", *Computational Mechanics*, 27, 2001 pp. 97–106.